



Aalborg Universitet

AALBORG UNIVERSITY  
DENMARK

## Voltage and Frequency Consensusability of Autonomous Microgrids over Fading Channels

Dehkordi, Nima Mahdian; Khorsandi, Amir; Baghaee, Hamid Reza; Sadati, Nasser; Moghaddam, Shahriar Shirvani; Guerrero, Josep M.

*Published in:*  
IEEE Transactions on Energy Conversion

*DOI (link to publication from Publisher):*  
[10.1109/TEC.2020.3005269](https://doi.org/10.1109/TEC.2020.3005269)

*Publication date:*  
2021

*Document Version*  
Accepted author manuscript, peer reviewed version

[Link to publication from Aalborg University](#)

*Citation for published version (APA):*  
Dehkordi, N. M., Khorsandi, A., Baghaee, H. R., Sadati, N., Moghaddam, S. S., & Guerrero, J. M. (2021). Voltage and Frequency Consensusability of Autonomous Microgrids over Fading Channels. *IEEE Transactions on Energy Conversion*, 36(1), 149-158. [9127122]. <https://doi.org/10.1109/TEC.2020.3005269>

### General rights

Copyright and moral rights for the publications made accessible in the public portal are retained by the authors and/or other copyright owners and it is a condition of accessing publications that users recognise and abide by the legal requirements associated with these rights.

- ? Users may download and print one copy of any publication from the public portal for the purpose of private study or research.
- ? You may not further distribute the material or use it for any profit-making activity or commercial gain
- ? You may freely distribute the URL identifying the publication in the public portal ?

### Take down policy

If you believe that this document breaches copyright please contact us at [vbn@aub.aau.dk](mailto:vbn@aub.aau.dk) providing details, and we will remove access to the work immediately and investigate your claim.

# Voltage and Frequency Consensusability of Autonomous Microgrids Over Fading Channels

Nima Mahdian Dehkordi, Amir Khorsandi, Hamid Reza Baghaee, *Member, IEEE*, Nasser Sadati, *Member, IEEE*, Shahriar Shirvani Moghaddam, *Senior Member, IEEE*, and Josep M. Guerrero, *Fellow, IEEE*

**Abstract**—In this paper, a novel cooperative secondary voltage/frequency control considering time-varying delays and noises in fading channels is presented for an autonomous alternating current (AC) voltage sourced-based converter (VSC)-based microgrid (MG), including inverter-interfaced distributed generations (DGs). Fading phenomenon makes complex random fluctuations on the voltage and frequency of every DG received from its neighbor DGs. In multi-agent cooperative systems, in addition to the total additive noise and time-variant delay, a multiplicative complex random variable is considered to model the main received signal and its replicas due to multipath propagation. The proposed consensus-based controller is designed by considering fading effects and examines mean square average-consensus considering time-varying delays and uncertainties of the communication system to regulate the voltage and frequency of autonomous AC MGs and provide an accurate real power-sharing. Therefore, by using the proposed protocols, the system sensitivity to fading is decreased, and consequently, the system reliability is increased. Several simulation case studies, such as comparison of the proposed method with previous methods, validate the robustness of our approach against the fading effect.

**Index Terms**—Consensusability, Fading channels, microgrids, multi-agent systems, secondary control, time-varying delay.

## I. INTRODUCTION

Indeed, the basic and most commonly used control structure for microgrids (MGs) is the hierarchical control that includes tertiary control (optimal operation), secondary control (restoration of both voltage and frequency), and primary control (droop control and primary stabilization) [1]. The reported secondary control methods are classified into the decentralized [2], centralized [3] (with low reliability), and distributed (with high reliability and low cost) [4]–[7].

The main goal of the primary control level is to provide power-sharing among distributed generations (DGs) by employing the droop control strategy. However, it adjusts both voltage and frequency deviations under the load demand [8]. The main objective of the secondary control level is the restoration of voltage and frequency [8]–[10]. Finally, at the point of common coupling (PCC), the tertiary controller is responsible for adjusting power-sharing between the MG and the upstream grid and providing power management between them. For the sake of regulating voltage and frequency of MG,

N. Mahdian is with the Faculty of Electrical Engineering, Shahid Rajaee Teacher Training University, Tehran, Iran (e-mail: nimamahdian@sru.ac.ir). A. Khorsandi and H. R. Baghaee are with the Department of Electrical Engineering, Amirkabir University of Technology, Tehran, Iran (a\_khorsandi@aut.ac.ir; hrbaghaee@aut.ac.ir). N. Sadati is with the Department of Electrical Engineering, Sharif University of Technology, Tehran, Iran (sadati@sharif.edu). S. Shirvani Moghaddam is with the Faculty of Electrical Engineering, Shahid Rajaee Teacher Training University, Tehran, Iran (e-mail: sh\_shirvani@sru.ac.ir). J. M. Guerrero is with the Department of Energy Technology, Aalborg University, Denmark (jgz@et.aau.dk).

the secondary control can offer cooperative characteristics so that an agent is considered for each DG unit that can cooperate with other agents [8].

Conventionally, the secondary control level employs a centralized structure, which requires a complicated point-to-point communication network with two-way communication links [11], [12]. This may increase the cost and system complexity and reduce the system reliability [11], [13], [14]. Recently, distributed cooperative secondary control strategies that use a sparse communication network have been proposed. Unlike the centralized method, in this method, each DG unit communicates with neighboring units. Therefore, the cost is reduced, and system reliability is improved [13], [15].

Unlike the conventional central controllers, the distributed secondary control schemes perform better when the communication latencies are considered [16]–[18]. Considering time delays in the switching communication network, by exploiting a distributed active/reactive power controller and voltage observer in a pinning-based voltage/frequency control scheme, a cooperative droop-based distributed controller has been presented for MGs [19]. This secondary control scheme has been finally employed for energizing nominal set points that are required for the primary control stage. It has been claimed that even with local and time-varying communication networks, each DG only requires intermittently communicating with its neighbors. Reference [20] presents a robust distributed secondary control (DSC) protocol by employing an iterative learning method to restore the voltages and frequency of the MG and provide proper real power-sharing. In the proposed control scheme, at the end of each step, the secondary control inputs are merely updated. The impact of communication time-delay on a proportional-integral (PI)-based centralized secondary frequency controller has been studied [21]. In [12], using a phase-locked loop (PLL) for acquiring frequency at bus loading and considering unknown and variable delay, a robust centralized secondary controller has been designed for the sake of frequency restoration.

In [22], using delay differential equations (DDEs), small-signal modeling of an islanded MG has been developed, and by applying a consensus-based controller that exploits a data network and graph theory, a distributed primary/secondary control system has been presented. Also, for secondary voltage and frequency restoration in an islanded MG, a distributed averaging PI-based controller has been proposed [23]. Also, a consensus-based frequency controller and distributed finite-time protocols have been proposed for voltage and frequency regulation, respectively [15]. In [24], [25], and [14], the authors have proposed the cooperative distributed methods by considering the noise in communication network among DGs. Besides, the problems of robustness against uncertainties,

stochastic disturbances, and fault resiliency of MGs have been addressed in [26]–[29] and [30], respectively.

The main insufficiency of the methods specified above is that the communication links among DGs are considered noise-free (ideal) channels without delay, whereas the channels are prone to noises and delays. However, in [31] the effects of having both constant delays and noises are considered. In multi-agent cooperative systems, fading may either be due to multipath propagation, weather (particularly rain), noises, delays, and shadowing from obstacles affecting the wave propagation. Fading makes every DG receives incomplete/imprecise information from its neighboring DGs.

Therefore, the main insufficiency of the work presented in [31] is that it only considers the constant time delays and noises. However, the above effects, such as rain, impose time-varying delays and severe noises.

The multipath phenomenon impacts the received signal as a linear distortion. In fading channels, besides additive Gaussian noise and delay, the received signals experience time-variant complex gains due to multipath phenomena. In other words, the received signals contain different coherent signals of the same source signals that their amplitudes and phases differ from each other. In this investigation, we assumed that no Doppler frequency, such as that for mobile wireless fading channels, could be seen. Hence, the coefficient matrix  $f_{ji}(t)$  is a time-variant random matrix, which its components are random variables with identically independent distributions (i.i.d) as complex stochastic processes including a Rayleigh (or Rice) distribution for its amplitude (positive random variable) and a uniform (or nonuniform) distribution for its phase [random variable in the interval  $(0, 2\pi)$ ]. Supposing that there exists block fading, the complex variable  $f_{ji}(t)$  does not change in the time of a block of data or one (or some) symbol ( $s$ ). In other words, the variation time of the channel is greater than the symbol time interval, which is a realistic assumption in the problem of this investigation.

The main drawbacks of the previous works are mainly in three aspects: 1) most of the reported distributed control strategies are considered to be ideal with noise-free communication among DGs, 2) [14], [24], others consider both noise and constant time delays or constant time delays [31]. However, in practice, fading may either be due to multipath propagation and shadowing, respectively from small and large obstacles besides noises and delays [32]. The above effects causes linear distortion, time-varying delays, and severe noises, leading to voltage and frequency instability of MGs.

To avoid the voltage and frequency instability caused by the fading effects, to the best of authors knowledge, this paper is the pioneer for proposing protocols that study mean square average-consensus to achieve accurate real power-sharing and regulating voltage and frequency in AC MGs over fading environments.

This paper proposes a fully distributed consensus secondary control for voltage and frequency regulation in islanded MGs considering fading effects. As far as we know, the main contributions of this paper which have not been presented yet, and are concisely provided in this paper as follows: 1) evaluate the effects of small-scale propagation phenomenon, namely,

multipath fading, on the performance of communication links and, 2) consider the time-varying model for communication link delays among the DG units.

## II. PROBLEM FORMULATION

We assume that DGs communicate with one another through a directed graph (digraph)  $G_r = (V_G, E_G, A_G)$ , where  $V_G$  is the number of DGs;  $E_G \subset V_G \times V_G$  is a set of DGs; and  $A_G \in R^{N \times N}$  is a weighted adjacent matrix with nonnegative elements  $a_{ij}$ . The communication link between two DGs is represented by the edge  $e_{ji} = (v_j, v_i)$  and exists if  $a_{ij} > 0$ . We assume that DGs have communication link with one another, i.e.  $a_{ii} = 0$ . Therefore, the adjacency matrix of the MG can be replaced by the communication layer topology. The neighbors of DG  $i$  is shown by  $N_i = \{j \in V_G : (i, j) \in E_G, j \neq i\}$ . In the MG system including  $N$  DGs, the voltages and frequencies of DGs play the role of followers, whereas their references represent the leader. The adjacency matrix of a leader is described as  $g = [g_1, g_2, \dots, g_N]^T \in R^N$ . If DG  $i$  receives the references,  $g_i = 1$ ; otherwise,  $g_i = 0$ . Moreover, the graph Laplacian matrix,  $L = [L_{ij}] \in R^{N \times N}$ , is defined as  $L_{ii} = \sum_{j \neq i} a_{ij}$  and  $L_{ij} = -a_{ij}$  [33].

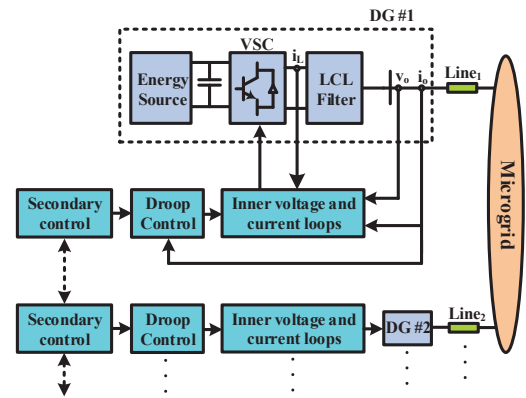


Fig. 1. General single line diagram of a VSC-based MG [31].

### A. Dynamic Model

The control of every unit should be expanded for maximum power point tracking for renewable energy resources by exploiting a low-bandwidth communication interface between local controllers and DGs to collect data needed for adaptive calculation of virtual resistances [34]. In case that a combination of dispatchable/non-dispatchable DGs are used in DC bus as main and auxiliary sources [35], or a reliable fast response energy storage unit such as super-capacitor is connected to a dispatchable source like Fuel Cell (FC) [36], hybrid energy resources can provide an almost constant DC-bus voltage for inverter. However, when non-dispatchable sources like wind generator, photovoltaic, or FC units are used, sometimes the installation of dispatchable units is not possible on account of their investment costs, although the reliability of such hybrid systems is almost much higher.

The following decentralized voltage and frequency droop controls are used for the primary level of the  $i^{th}$  DG (the associated block is specified in Fig. 1)

$$\begin{aligned}\omega_i &= \omega_{ni} - m_{P_i} P_i \\ v_{mag,i} &= V_{ni} - n_{Q_i} Q_i,\end{aligned}\quad (1)$$

where  $\omega_i$  and  $v_{mag,i}$  represent the nominal values of voltage and frequency provided for the inner controllers, respectively.  $m_{P_i}$  and  $n_{Q_i}$  are the voltage and frequency droop coefficients.  $V_{ni}$  and  $\omega_{ni}$  are the setpoints for the primary level in (1). Also,  $P_i$  and  $Q_i$  are the real and reactive powers of the inverter.

By applying feedback linearization to (1), the model of the system is represented by

$$\dot{\omega}_i = \dot{\omega}_{ni} - m_{P_i} \dot{P}_i = u_{\omega_i} \quad (2)$$

$$\dot{v}_{mag,i} = \dot{V}_{ni} - n_{Q_i} \dot{Q}_i = u_{v_i}, \quad (3)$$

where  $u_{\omega_i}$  and  $u_{v_i}$  are auxiliary control inputs. Equations (2) and (3) represent the dynamic system to compute the control inputs  $\omega_{ni}$  and  $V_{ni}$ . It follows from (2) and (3) that the voltage/frequency restoration of an MG including  $N$  DGs is presented by the following tracking synchronization problem:

$$\dot{\omega}_i = u_{\omega_i}, i = 1, 2, \dots, N \quad (4)$$

$$\dot{v}_{mag,i} = u_{v_i}, i = 1, 2, \dots, N. \quad (5)$$

Following from references [13], [23], cooperation among inverters is achieved under the following voltage and frequency error terms

$$e_{v_i} = \sum_{j \in N_{ci}} (v_i(t) - v_j(t)) + g_i(v_i(t) - v_{ref}) \quad (6)$$

$$e_{\omega_i} = \sum_{j \in N_{ci}} (\omega_i(t) - \omega_j(t)) + g_i(\omega_i(t) - \omega_{ref}) \quad (7)$$

in which  $v_i$  and  $v_j$ , along with  $\omega_i$  and  $\omega_j$ , are the  $i^{th}$  and  $j^{th}$  inverter's output voltages and frequencies neighboring on the graph, respectively;  $g_i$  is the voltage/frequency pinning gain, which is nonzero for the DG that has access to the reference voltage/frequency values  $v_{ref}$  and  $\omega_{ref}$ ; and  $N_{ci}$  represents the communication neighborhood set of the  $i^{th}$  protocol. The abovementioned cooperative errors assume that  $i^{th}$  DG obtains information from its neighbors accurately, i. e., it neglects fading in communication channels. To overcome the difficulties mentioned above, inspired by [33], we propose a distributed consensus-based noise-resilient secondary control for the restoration of the voltage and frequency in an islanded MG considering time delays in communication channels.

### III. VOLTAGE RESTORATION OVER FADING CHANNELS

The secondary voltage/frequency control selects  $V_{ni}$  and  $\omega_{ni}$  in (1) to synchronize the output voltages and frequencies of each inverter to the nominal values. To this end, each inverter exchanges data only with its neighbors on a communication graph. Motivated by [33], to restore the voltages of MG, we propose the cooperative consensus-based protocols considering fading as:

$$u_{v_i} = c(t) \sum_{j \in N_{ci}} a_{ij} [y_{ji} - v_{mag,i}(t - \tau_{ij}(t))], \quad i \in l, \quad (8)$$

where  $y_{ji} = f_{ji}(t)v_{mag,j}(t - \tau_{ij}(t)) + \sigma_{ji}\dot{w}_{ji}(t)$ ,  $v_{mag,i}$  represents the amplitude of  $v_i$ ,  $\dot{w}_{ji}(t)$  represents the independent standard white noise,  $\sigma_{ji} \geq 0$  represents the noise intensity,  $\tau_{ij}(t)$  indicates time-varying communication delays,  $f_{ji}(t)$  denotes complex Gaussian stochastic process to show the effect of multipath fading, and  $c(t)$  represents a piecewise continuous function satisfying

$$\int_0^\infty c(s)ds = \infty \quad \text{and} \quad \int_0^\infty c^2(s)ds < \infty. \quad (9)$$

The signal to noise ratio (SNR) and ergodic capacity of the links between the main node and neighbors considering the effect of multipath fading on the voltage are analyzed in Appendix. The main feature of the proposed method is that besides the additive noises and time-varying delays, it considers Rayleigh and Rician fading components [37] by using complex Gaussian coefficients in (8).

It should be noted that  $c(t)$  attenuates the adverse effects of noise as  $t \rightarrow \infty$ . Let  $e = [e_1^T, \dots, e_n^T]^T$ . Therefore, the global error vector  $e$  can be defined as

$$e = (L \otimes I_n) \begin{bmatrix} v_{mag,1} - v_{ref} \\ \vdots \\ v_{mag,N} - v_{ref} \end{bmatrix}, \quad (10)$$

where  $\otimes$  and  $I_n$  represent the Kronecker product and unit matrix of size  $n$ , respectively. Substituting for  $u_{v_i}$  from (8) into (5), yields

$$de(t) = c(t) [-Le(t - \tau(t))dt + \Theta dW(t)], \quad (11)$$

where  $\Theta \in R^{n \times n^2}$  represents a constant matrix represented by  $\Theta = \text{diag}(\Theta_1, \dots, \Theta_n)$  in which  $\Theta_i = [a_{i1}\sigma_{1i} \ a_{i2}\sigma_{2i} \ \dots \ a_{in}\sigma_{ni}]$ , and  $W(t) \in R^{n^2}$  represents a Wiener process. In the following, we introduce a displacement vector as

$$\delta(t) = e(t) - \mathbf{1}\alpha(t) = (1 - J)e(t), \quad (12)$$

where  $\mathbf{1}$  indicates the column vector with elements of one;  $I$  represents  $n \times n$  identity matrix;  $\alpha(t) = \text{avg}(x(t)) = \frac{1}{n} \mathbf{1}^T x(t) = \frac{1}{n} \sum_{i=1}^N x_i(t)$ ; and  $J = \frac{1}{n} \mathbf{1}\mathbf{1}^T$ . It can be easily seen that

$$\mathbf{1}^T \delta(t) = \sum_{i=1}^N e_i(t) - n\alpha(t) = 0, \forall t \geq 0. \quad (13)$$

For as much as both  $\mathbf{1}^T L$  and  $L\mathbf{1}$  are vectors; therefore, the dynamics of  $\delta(t)$  is represented by

$$d\delta(t) = c(t) [-L\delta(t - \tau(t))dt + (I - J)\Theta dW(t)]. \quad (14)$$

The above-mentioned results are presented below.

*Theorem 3.1:* The continuous protocol

$$\begin{aligned}V_{ni} &= \int (u_{v_i} + n_{Q_i} \dot{Q}_i) dt, \quad i = 1, 2, \dots, N \\ u_{v_i} &= c(t) \sum_{j \in N_{ci}} a_{ij} [y_{ji} - v_{mag,i}(t - \tau_{ij}(t))]\end{aligned}\quad (15)$$

causes the voltage of DG,  $v_{mag,i}$ , synchronizes with  $v_{ref}$  irrespective of time-varying delays and noises in communication networks over fading channels. Moreover, we have

$$\dot{Q}_i = -\omega_c Q_i + \omega_c (v_{oqi} i_{odi} - v_{odi} i_{oqi}). \quad (16)$$

*Proof:* The proof is similar to the Theorem 3.1 in the reference [33]. ■

It should be noted that the control gain  $c(t)$  is calculated from the beginning of the event [e.g. disturbances, load changes, communication network changes, and plug and play (P&P) of DGs].

#### IV. FREQUENCY RESTORATION OVER FADING CHANNELS

In this section, we design a consensus-based frequency restoration method by selecting a proper protocol,  $\omega_{ni}$ , in (4) to adjust the frequency of DGs,  $\omega_i$ , to its nominal value  $\omega_{ref}$ , while considering the effects of fading. We should remark that the droop control shares real power among DGs according to equation (17); So, subsequent to the application of consensus method, the accuracy of the real power-sharing is guaranteed:

$$\frac{P_j}{P_i} = \frac{m_{pi}}{m_{pj}}, \quad \forall i, j \in N. \quad (17)$$

We assume that DGs communicate with one another through a fading-affected directed graph  $G_r$ . As a result, the proposed restoration method designs  $\omega_{ni}$  in (1) so that  $\omega_i \rightarrow \omega_{ref}$  and  $m_{pk} P_k \rightarrow m_{pi} P_i, \forall i$ . Similar to the voltage restoration layer, we suggest the following consensus-based frequency restoration considering fading,  $u_{\omega i}$ , based on its neighbors' information on the communication graph; therefore, each DG's angular frequency,  $\omega_i$ , synchronizes with global reference,  $\omega_{ref}$ , while guaranteeing the real power-sharing accuracy:

$$u_{\omega i} = c(t) \left( \sum_{j \in N_{ci}} a_{ij} [y_{ji} - \omega_i(t - \tau_{ij}(t))] + \sum_{j \in N_{ci}} a_{ij} [\gamma_{ji} - m_{pj} P_i(t - \tau_{ij}(t))] \right), \quad (18)$$

where  $y_{ji} = f_{ji}(t) \omega_j(t - \tau_{ij}(t)) + \sigma_{ji} \dot{w}_{ji}(t)$ ,  $\gamma_{ji} = f_{ji}(t) m_{pj} P_j(t - \tau_{ij}(t)) + \sigma_{ji} \dot{w}_{ji}(t)$ . The second term of (18) is for preserving the real power-sharing after implementing the proposed protocols, even if the communication network fails. Based on equations (2) and (4), we can write  $\omega_{ni}$  as:

$$\omega_{ni} = \int u_{\omega i}, \quad i = 1, 2, \dots, N. \quad (19)$$

The above-mentioned results are presented in the form of the following theorem.

*Theorem 4.1:* The consensus method (19) undertakes that the DG's output frequency,  $\omega_{ni}$  synchronizes with  $\omega_{ref}$  irrespective of time-varying delays and noises in fading channels.

*Proof:* The proof is similar to the Theorem 3.1 in the reference [33]. ■

Because fading in the communication channels are unavoidable, compared with the existing distributed control methods, the proposed method considers time-varying delays and noises, and has better noise cancellation and robustness against fading in communication channels. As is seen from (18), the protocol

$u_{\omega i}$  contains two parts; the first part results in steady-state tracking of the frequency nominal setpoint (i.e.,  $\omega_i \rightarrow \omega_{ref}$ ), despite fading, and the second one guarantees real power-sharing accuracy (i.e.,  $m_{pj} P_j \rightarrow m_{pi} P_i$ ).

The main feature of our method is that it considers the fading channels, time-varying delays, and noises in a joint manner. Moreover, the mechanism of how the proposed method can reduce the impact of fading is illustrated in proofs of Theorems 3.1 and 4.1. In fact, our proposed cooperative control strategy makes use of the states of each DG and its neighbors. To attenuate the fading effects, the time-varying gain vector  $c(t)$  is used to compensate for inaccurate relative states (see the proof of Theorems 3.1 and 4.1). Furthermore, it does not matter what kind of adjacency matrix is selected. The time-varying gain  $c(t)$  is selected in such a way that it deals with different dynamics. Our presented protocols do not require heavy computations or difficult operations. Therefore, the proposed method does not impose a heavy computational burden or practical limitations.

#### V. SIMULATION RESULTS

To show the effectiveness, authenticity, robustness, and accuracy of the proposed cooperative distributed secondary controller and its consensusability over fading channels, an MG with multiple DG units [19] is simulated under different simulation scenarios in MATLAB/Simulink software environment, and the results are verified by comparing with previously-reported conventional distributed control technique [13]. The time-varying communication delay is considered  $0.2 \sin(2t)$  s. The MG system parameters are given in [19]. We have obtained simulation results that consider practical conditions. From a practical point of view, the following are considered:

- 1) The line loss has been considered in our calculation.
- 2) A system with time-varying communication delays is simulated.
- 3) The DG units' local controllers are digitally implementable, which makes them ideal for real-time applications.
- 4) The switching of VSCs is modeled in detail.
- 5) We have considered a time-delay on PWM controller output, before being applied to the switches.
- 6) The signal sampling delay has been taken into account before processing the VSCs control loops.
- 7) The proposed controller does not require heavy computations. Therefore, for practical implementation, the computational complexity of the proposed control scheme would not be a significant concern.

Considerations for the hardware implementation of this algorithm is similar to the control signals which are used in various studies. Still, it has some features which make it robust against unknown noises and time-varying delays. The proposed algorithm uses adaptation laws in its implementation that are made of measurable signals such as state estimation errors among DG units. Thus, it can be easily implemented on digital signal processing (DSP) or field-programmable gate array (FPGA) chips and linked with experimental and/or real-time simulator setups.

When the proposed strategy is used for real-life practical MGs, the algorithm can be transformed into the equivalent discrete form and implemented on DSP and FPGA chips, or micro-controllers for experimental setups and real-time verification in the form of controller hardware in the loop (CHIL) via online closed-loop real-time digital simulators (RTDSs) [38]. The essential item for the experimental or real-time implementation is choosing the sampling frequency and the processing speed of the processors. The proposed voltage and frequency controllers must be supported by a local communication network that can be implemented by a transmission control protocol/internet protocol (TCP/IP) communication protocol with optical fiber links [39], [40]. The sampling time of the secondary controller can be chosen to be much larger than the sampling time of the communication network. Communication links contain an intrinsic delay (for example, around 1 ms for optical fiber links [40]).

For reactive power, it is worth mentioning that the proposed control strategy does not be affected by line losses. The only essential item that should be considered is that due to the impedance effect of transmission lines, both accurate reactive power sharing and voltage regulation can not be achieved simultaneously [17]. Therefore, precise voltage regulation results in significant errors in reactive power-sharing. Conversely, accurate reactive power sharing leads to poor voltage regulation. Thus, a trade off should be made between voltage regulation and reactive power sharing accuracy. In this paper, we have just focused on the secondary voltage and frequency control.

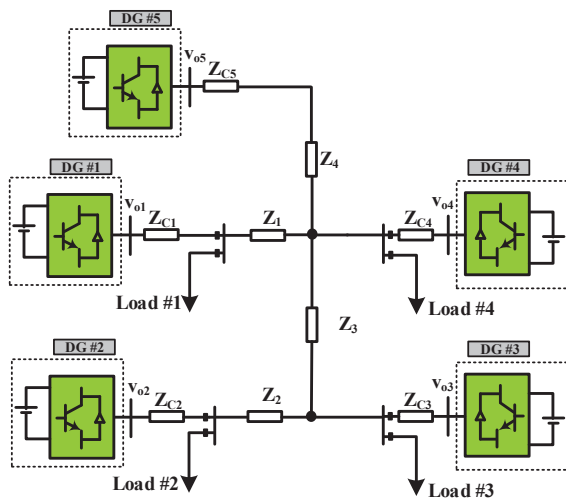


Fig. 2. Topology of the MG system [19].

### A. Performance Evaluation Over Fading Channels

This section validates the performance and the consensus-ability of the protocols over fading channels with the following simulation scenarios:

- 1)  $t = 0.0$  s: (initialization of simulation). The voltage and frequency droop controllers are applied, and Load #6 is out of the service.

- 2)  $t = 0.5$  s: The consensus-based controller is activated.
- 3)  $t = 2$  s: 100% increment in Load #1.
- 4)  $t = 2.7$  s: White Gaussian noise with  $\sigma^2 = 0.1$  is added.
- 5)  $t = 3.2$  s: Time-varying delay ( $0.2 \sin(2t)$  s) is considered.
- 6)  $t = 3.8$  s: DG #5 is disconnected (plugged out).
- 7)  $t = 4.8$  s: DG #5 is reconnected (plugged in).

The system starts with the primary controller. After applying the proposed controller at  $t = 0.5$  s, and load step change at  $t = 2$  s, the fading communication channels are affected by an additive noise with  $\sigma^2 = 0.1$ . Then, the time-varying delay  $0.2 \sin(2t)$  s is considered after  $t = 3.2$  s. Figs. 3 and 4 show that the consensus protocols can restore both voltage and frequency after a load change disturbance has occurred. In the next scenario, both noise and time-varying delays are considered in communication channels. We observe that the distributed protocols can restore the voltage and frequency of MG in finite time. Finally, when the DG #5 plugged out at  $t = 3.8$  s and then plugged in again at  $t = 4.8$  s, the proposed control scheme responds well against a large-signal disturbance, namely outage and reconnection of DG unit. Consequently, robust performance against noises, time-varying delays, and P&P functionality of MG is realized, and robust stability is provided.

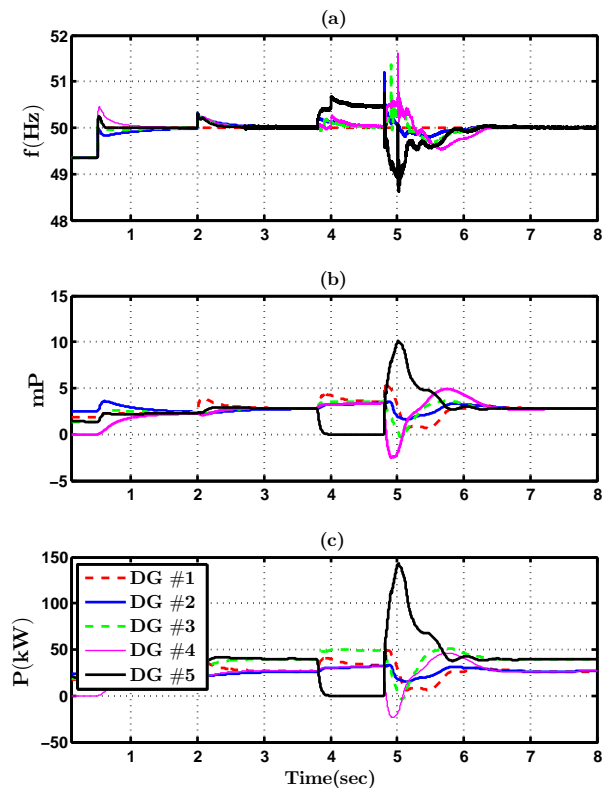


Fig. 3. a) frequencies, b) real power ratios, and c) output real power of DG units over fading channels.

For the realization of voltage and frequency regulation and active/reactive power-sharing and consensus-ability of MG over fading channels, we need to implement primary controllers and inner control loops (including virtual impedance), which is not

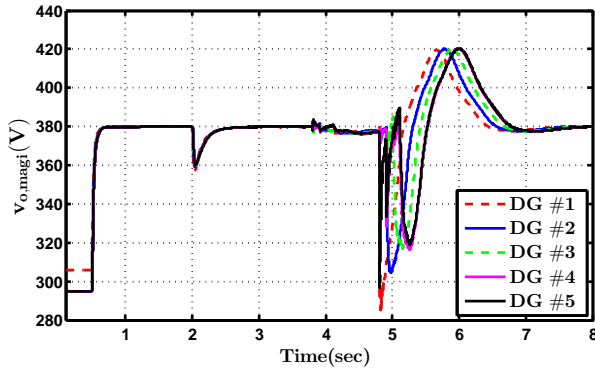


Fig. 4. PCC voltages of DG units over fading channels.

the subject of this paper. However, in the future, we will extend our control strategy to also support the mentioned case. By using the proposed consensus secondary controller, we have evaluated the performance of the system for several scenarios and compared the evaluation results with the ones reported earlier. Simulation results effectively prove that although we have not considered the dynamics of the primary controller, the proposed control scheme does not deteriorate reactive power-sharing and active/reactive power-sharing is realized.

### B. Noise and Communication Delay Changes in Fading Channels

In this section, the authenticity, robustness, and resilience of the proposed consensus secondary controller when delays and noise are changed, will be discussed. Here, the noise variance varies from  $\sigma^2 = 0.1$  to  $\sigma^2 = 0.8$  (eight times), and also the communication delay from  $0.2 \sin(2t)$  s to  $0.3 \sin(2t)$  s. Then, the simulation scenario of subsection VI-A is repeated. Again, we observe from Figs. 5 and 6 that, both the voltage and frequency are restored irrespective of the higher noise levels and communication time-varying delays in fading channels. Because fading in communication channels are unavoidable, compared with the existing distributed control methods, the proposed method has better noise cancellation and robustness against time-varying delays in communication channels. As seen from (19), the protocol  $u_{\omega_i}$  contains two parts: the first part of protocol results in tracking of the nominal frequency in steady-state (i.e.,  $\omega_i \rightarrow \omega_{ref}$ ), despite time-varying delays and noises in fading channels, and the second one guarantees real power-sharing accuracy (i.e.,  $m_{pj}P_j \rightarrow m_{pi}P_i$ ). Moreover, the real powers shared among the DGs according to droop coefficients, as depicted in Figs. 5 and 6.

### C. Communication Network Change in Fading Channels

In this section, to evaluate the robustness of our proposed protocols against the change of communication network in the MG, the topology of the communication graph changes from  $G_1$  [Fig. 7 (a)] to  $G_2$  [Fig. 7 (b)]. Then, we repeat the study A with the same simulation scenario. Again, we observe from Figs. 8 and 9 that, the voltage and frequency are restored irrespective of the communication network changes, higher values of noise, communication time-varying delay, and P&P functionality of the MG in fading channels.

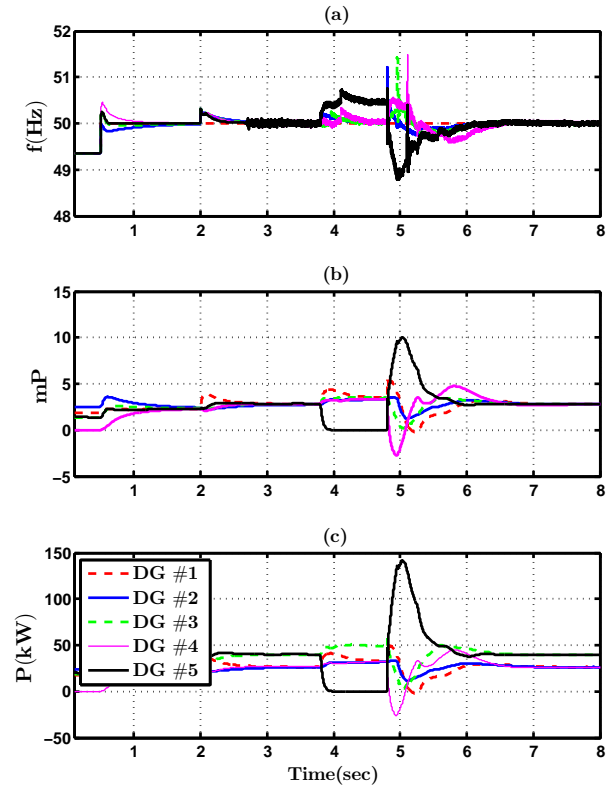


Fig. 5. Change of additive noise and communication delay in fading networks: a) frequencies, b) real power ratios, and c) output real powers of DG units over fading channels.

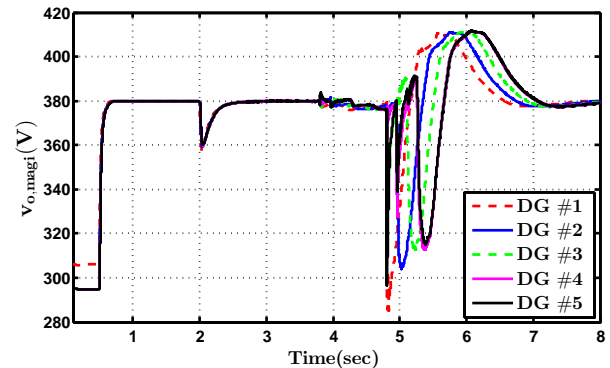


Fig. 6. Change of additive noise and communication delay in fading networks: PCC voltages of DG units over fading channels.

### D. Comparison with a Previously-Reported Control Technique

The performance of the proposed secondary controller is compared with the distributed technique presented in [13]. We perform the simulation scenario of Subsection VI-A by using the protocols proposed in [13]. The results presented in Figs. 10 and 11 show that when the conventional method [13] is used in the presence of the noise with  $\sigma^2 = 0.1$ , the voltage and frequency waveforms become unstable. However, our consensus protocols, as mentioned in Subsection VI-B, have desirable performance despite higher noise variance values and time-varying delay in fading channels. As compared with the distributed controller proposed in [14], the proposed protocols

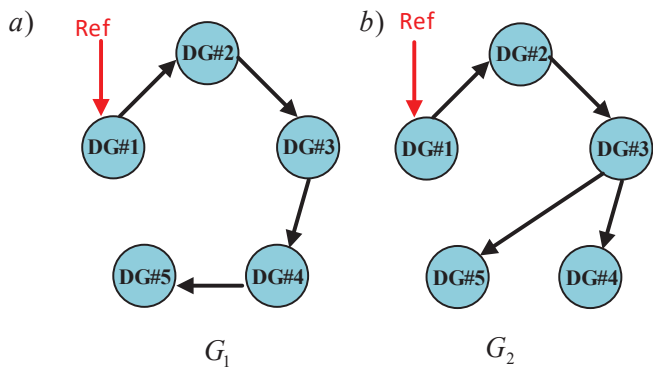


Fig. 7. Topology of communication graphs: a) old topology and b) new topology.

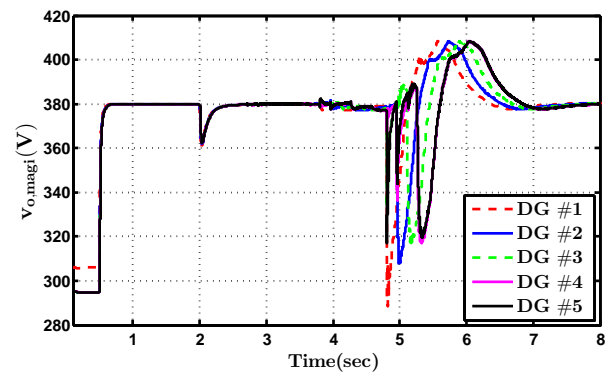


Fig. 9. Communication network change in fading channels: PCC voltages of DG units over fading channels.

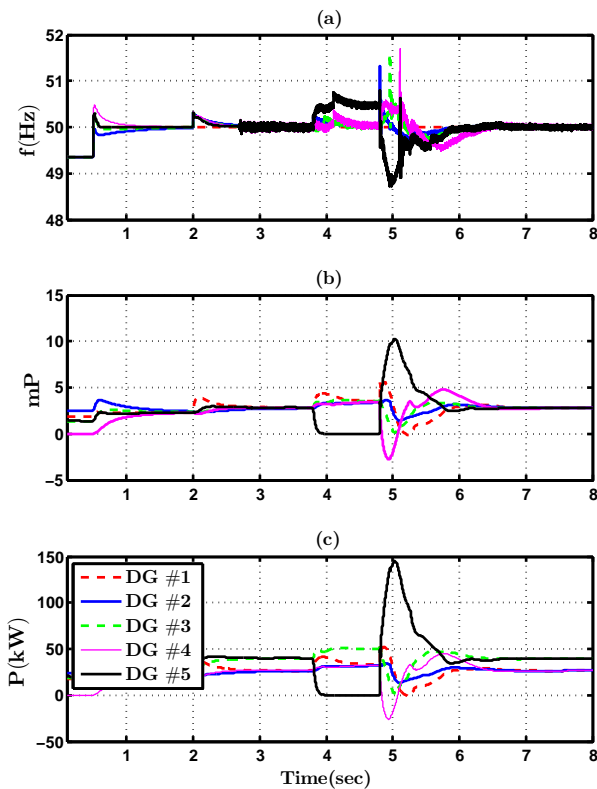


Fig. 8. Communication network change in fading channels: a) frequencies, b) real power ratios, and c) output real powers of DG units over fading channels.

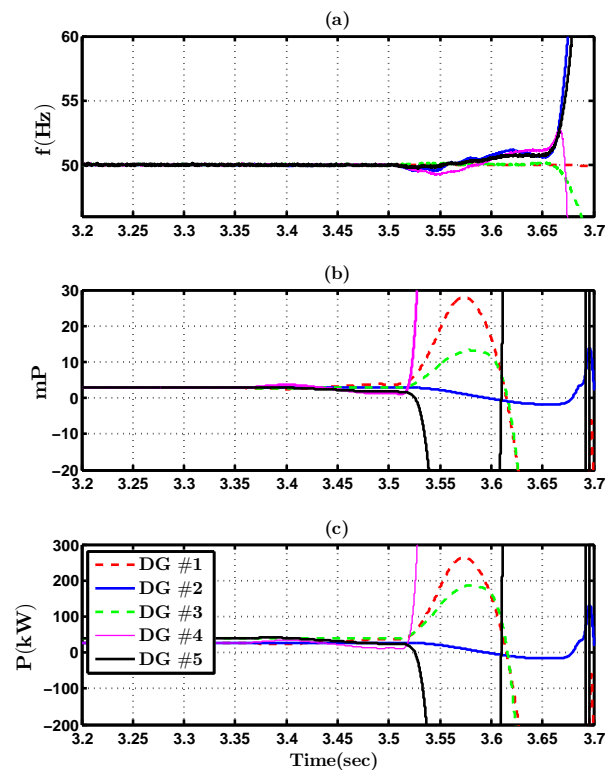


Fig. 10. a) frequencies, b) real power ratios, and c) output real powers of DG units considering fading, using the distributed method in [13].

rejects the adverse effects of both time-varying delays and noises in fading communication channels.

## VI. CONCLUSION

In this paper, a new consensus-based secondary voltage and frequency control scheme has been proposed for voltage and frequency restoration of an autonomous inverter-based MG that takes the fading into account. The consensus protocols were proposed considering time-varying delays and noises in fading channels. In multi-agent cooperative systems, fading may either be due to multipath propagation and shadowing due to large obstacles. As it was observed, the proposed

method reaches mean square consensus and, therefore, the secondary voltage and frequency protocols are synchronized to their nominal values irrespective of time-varying delays and noises in fading channels. Finally, to verify the authenticity, effectiveness, and robustness of the proposed control scheme, we carried out extensive time-domain digital simulations in MATLAB/Simulink. The results show that the voltage and frequency of the MG are robustly restored to their reference values irrespective of time-varying delays and noises. In addition, an accurate real power-sharing and P&P functionality of DG units were achieved.



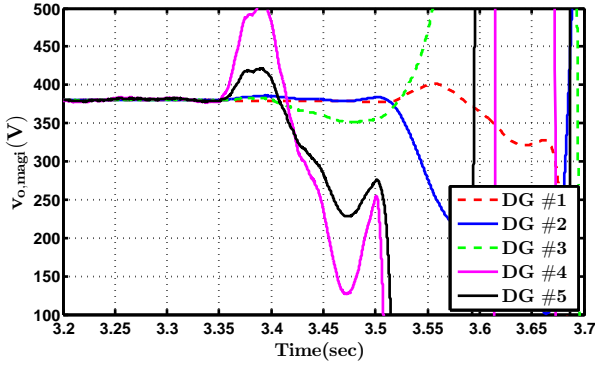


Fig. 11. PCC voltages of DG units considering fading, using the distributed method in [13].

### APPENDIX

Referring to (8), the received signal in node  $i$  is given as

$$v_{ji}(t) = y_{ji} - v_{mag,i}(t - \tau_{ij}(t)) = f_{ji}(t) v_{mag,j}(t - \tau_{ij}(t)) + \sigma_{ij}(t) \dot{\omega}_{ji}(t) - v_{mag,i}(t - \tau_{ij}(t)). \quad (20)$$

It is in the form of a two-term equation as (20), which the first term is signal, and the second term is the additive noise.

$$v_{ji}(t) = s_{ji}(t) + n_{ji}(t), \quad (21)$$

where, the signal  $s_{ji}(t)$  and noise  $n_{ji}(t)$  are as (22) and (23), respectively.

$$s_{ji}(t) = f_{ji}(t) v_{mag,j}(t - \tau_{ij}(t)) - v_{mag,i}(t - \tau_{ij}(t)), \quad (22)$$

$$n_{ji}(t) = \sigma_{ij}(t) \dot{\omega}_{ji}(t). \quad (23)$$

SNR for each link between neighbor and main nodes,  $i$  and  $j$ , is as (24).

$$snr_{ji} = \frac{E\{s_{ji}^2\}}{E\{n_{ji}^2\}} = \frac{E\{v_{mag,j}^2\} \cdot |f_{ji}|^2 + E\{v_{mag,i}^2\}}{E\{n_{ji}^2\}}. \quad (24)$$

Considering valid assumptions for wired and wireless links, assume that

$$E\{v_{mag,j}\} = E\{v_{mag,i}\} = 0 \quad (25)$$

$$Var\{v_{mag,j}\} = Var\{v_{mag,i}\} = \sigma_v^2 \quad (26)$$

$$E\{n_{ji}\} = 0, \quad (27)$$

and

$$E\{v_{mag,j}, v_{mag,i}\} = 0, \quad (28)$$

which means that  $v_{mag,j}$  and  $v_{mag,i}$  are uncorrelated. Therefore,

$$E\{v_{mag,j}^2\} = E\{v_{mag,i}^2\} = \sigma_v^2 \quad (29)$$

$$E\{n_{ji}^2\} = \sigma_{ij}^2. \quad (30)$$

Finally, it is given that

$$snr_{ji} = \frac{\sigma_v^2(1 + |f_{ji}|^2)}{\sigma_{ij}^2} = \frac{2\sigma_v^2}{\sigma_{ij}^2} \left( \frac{1 + |f_{ji}|^2}{2} \right). \quad (31)$$

The term  $\left(\frac{1 + |f_{ji}|^2}{2}\right)$  shows the effect of the multipath fading and the term  $\frac{2\sigma_v^2}{\sigma_{ij}^2}$  is the SNR for free-fading scenario.

Due to multipath fading, SNR depends on the fading gain,  $|f_{ji}|^2$ , that changes from one data block to another one, randomly. It means that considering block fading for each link between node  $i$  and node  $j$ , the instantaneous fading component changes SNR. The average SNR is as follows:

$$s\bar{n}r_{ji} = \frac{2\sigma_v^2}{\sigma_{ij}^2} E \left\{ \frac{1 + |f_{ji}(t)|^2}{2} \right\} = \frac{2\sigma_v^2}{\sigma_{ij}^2} \left( \frac{1 + E\{|f_{ji}(t)|^2\}}{2} \right). \quad (32)$$

For Rayleigh fading channels,

$$s\bar{n}r_{ji} = \frac{2\sigma_v^2}{\sigma_{ij}^2} \left( \frac{1 + 2\delta^2}{2} \right), \quad (33)$$

where,

$$\left\{ \begin{array}{l} f_{|f_{ji}|}(|f_{ji}|) = \frac{|f_{ji}|}{\delta^2} e^{-\frac{|f_{ji}|^2}{2\delta^2}} \\ E\{|f_{ji}|^2\} = \sqrt{\frac{\pi}{2}} \delta \\ Var(|f_{ji}|^2) = (2 - \frac{\pi}{2})\delta^2 \end{array} \right\}. \quad (34)$$

Hence,  $E\{|f_{ji}|^2\} = 2\delta^2$ .

For Rician fading channels,

$$s\bar{n}r_{ji} = \frac{2\sigma_v^2}{\sigma_{ij}^2} \left( \frac{1 + 2\delta^2 + s^2}{2} \right), \quad (35)$$

where,

$$\left\{ \begin{array}{l} f_{|f_{ji}|}(|f_{ji}|) = \frac{|f_{ji}|}{\delta^2} I_0 \left( \frac{|f_{ji}| \cdot s}{\delta^2} \right) e^{-\frac{|f_{ji}|^2 + s^2}{2\delta^2}} \\ E\{|f_{ji}|^2\} = \sqrt{\frac{\pi}{2}} \delta e^{-\frac{K}{4}} \sqrt{(1 + K)I_0\left(\frac{K}{2}\right) + KI_1\left(\frac{K}{2}\right)} \\ Var(|f_{ji}|^2) = 2\delta^2 + s^2 - \frac{\pi}{2}\delta^2 e^{-\frac{K}{2}} \left[ (1 + K)I_0\left(\frac{K}{2}\right) + KI_1\left(\frac{K}{2}\right) \right] \end{array} \right\}, \quad (36)$$

where,  $I_0(\cdot)$  and  $I_1(\cdot)$  are zero-order and first-order modified Bessel functions, respectively. The Rician  $K$ -factor is defined as:

$$K = \frac{s^2}{2\delta^2}. \quad (37)$$

Hence,  $E\{|f_{ji}|^2\} = 2\delta^2 + s^2$ .

Although the average SNR is increased for large values of fading variances, but the desired signal is distorted. In other words, the proper metric to evaluate the performance of each link should be changed to ergodic capacity defined as (38).

$$\bar{C}_{ji} = \int_0^\infty C_{ji} f_{|f_{ji}|}(x) dx, \quad (38)$$

knowing that Shannon-Hartley capacity is given by

$$C_{ji}(x) = B \log_2(1 + snr_{ji}(x)). \quad (39)$$

Using (31) and (39),

$$\bar{C}_{ji} = B \int_0^\infty \log_2 \left( 1 + \frac{2\sigma_v^2}{\sigma_{ij}^2} \left( \frac{1 + x^2}{2} \right) \right) f_{|f_{ji}|}(x) dx. \quad (40)$$

For fading-free scenario, we have

$$\begin{aligned}\bar{C}_{ji} &= B \int_0^\infty \log_2 \left( 1 + \frac{2\sigma_v^2}{\sigma_{ij}^2} \left( \frac{1+x}{2} \right) \right) f_{|f_{ji}|}(x) dx \\ &= B \log_2 \left( 1 + \frac{2\sigma_v^2}{\sigma_{ij}^2} \right) \int_0^\infty f_{|f_{ji}|}(x) dx \\ &= B \log_2 \left( 1 + \frac{2\sigma_v^2}{\sigma_{ij}^2} \right)\end{aligned}\quad (41)$$

which means that the ergodic capacity [41],  $\bar{C}_{ji}$ , equals to capacity for free-fading links. This value is an upper bound for fading links. Therefore, the ergodic capacities for Rayleigh and Rician fading links are as (42) and (43), respectively, both lower than the upper bound evaluated in the free-fading scenario.

$$\bar{C}_{ji} = B \int_0^\infty \log_2 \left( 1 + \frac{2\sigma_v^2}{\sigma_{ij}^2} \left( \frac{1+x^2}{2} \right) \right) \frac{x}{\delta^2} e^{-\frac{x^2}{2\delta^2}} dx \quad (42)$$

$$\bar{C}_{ji} = B \int_0^\infty \log_2 \left( 1 + \frac{2\sigma_v^2}{\sigma_{ij}^2} \left( \frac{1+x^2}{2} \right) \right) \frac{x}{\delta^2} I_0 \left( \frac{x.s}{\delta^2} \right) e^{-\frac{x^2+s^2}{2\delta^2}} dx. \quad (43)$$

The similar analysis is valid for the SNR and ergodic capacity of the links between the main node and neighbors considering the effect of multipath fading on the frequency (equation 18).

## REFERENCES

- [1] J. M. Guerrero, J. C. Vasquez, J. Matas, L. G. de Vicuna, and M. Castilla, "Hierarchical control of droop-controlled AC and DC microgrids—a general approach toward standardization," *IEEE Trans. Ind. Electron.*, vol. 58, no. 1, pp. 158–172, Jan. 2011.
- [2] Y. Mohamed and E. El-Saadany, "Adaptive decentralized droop controller to preserve power sharing stability of paralleled inverters in distributed generation microgrids," *IEEE Trans. Power Electron.*, vol. 23, no. 6, pp. 2806–2816, 2008.
- [3] A. G. Tsikalakis and N. D. Hatziargyriou, "Centralized control for optimizing microgrids operation," *IEEE Trans. Energy Convers.*, vol. 23, no. 1, pp. 241–248, Mar. 2008.
- [4] Q. Shafiee, C. Stefanovic, T. Dragicevic, P. Popovski, J. C. Vasquez, and J. M. Guerrero, "Robust networked control scheme for distributed secondary control of islanded microgrids," *IEEE Trans. Ind. Electron.*, vol. 61, no. 10, pp. 5363–5374, Oct. 2014.
- [5] C. Li, E. A. A. Coelho, T. Dragicevic, J. M. Guerrero, and J. C. Vasquez, "Multiagent-based distributed state of charge balancing control for distributed energy storage units in AC microgrids," *IEEE Trans. Ind. Appl.*, vol. 53, no. 3, pp. 2369–2381, May 2017.
- [6] C. Zhao, W. Sun, J. Wang, Q. Li, D. Mu, and X. Xu, "Distributed cooperative secondary control for islanded microgrid with markov time-varying delays," *IEEE Trans. Energy Convers.*, pp. 1–1, 2019.
- [7] W. Yuan, Y. Wang, X. Ge, X. Hou, and H. Han, "A unified distributed control strategy for hybrid cascaded-parallel microgrid," *IEEE Trans. Energy Convers.*, pp. 1–1, 2019.
- [8] M. Chen, X. Xiao, and J. M. Guerrero, "Secondary restoration control of islanded microgrids with decentralized event-triggered strategy," *IEEE Trans. Ind. Informat.*, vol. PP, no. 99, pp. 1–1, 2017.
- [9] N. L. Daz, J. C. Vasquez, and J. M. Guerrero, "A communication-less distributed control architecture for islanded microgrids with renewable generation and storage," *IEEE Trans. Power Electron.*, vol. 33, no. 3, pp. 1922–1939, Mar. 2018.
- [10] Q. Li, C. Peng, M. Wang, M. Chen, J. M. Guerrero, and D. Abbott, "Distributed secondary control and management of islanded microgrids via dynamic weights," *IEEE Trans. Smart Grid*, vol. PP, no. 99, pp. 1–1, 2018.
- [11] A. Bidram and A. Davoudi, "Hierarchical structure of microgrids control system," *IEEE Trans. Smart Grid*, vol. 3, no. 4, pp. 1963–1976, Dec. 2012.
- [12] C. Ahumada, R. Crdenas, D. Sez, and J. M. Guerrero, "Secondary control strategies for frequency restoration in islanded microgrids with consideration of communication delays," *IEEE Trans. Smart Grid*, vol. 7, no. 3, pp. 1430–1441, May 2016.
- [13] A. Bidram, A. Davoudi, F. L. Lewis, and Z. Qu, "Secondary control of microgrids based on distributed cooperative control of multi-agent systems," *IET Gener Transm Dis.*, vol. 7, no. 8, pp. 822–831, Aug. 2013.
- [14] S. Abhinav, I. Schizas, F. Lewis, and A. Davoudi, "Distributed noise-resilient networked synchrony of active distribution systems," *IEEE Trans. Smart Grid*, vol. PP, no. 99, pp. 1–1, 2017.
- [15] F. Guo, C. Wen, J. Mao, and Y. D. Song, "Distributed secondary voltage and frequency restoration control of droop-controlled inverter-based microgrids," *IEEE Trans. Ind. Electron.*, vol. 62, no. 7, pp. 4355–4364, Jul. 2015.
- [16] Q. Shafiee, J. M. Guerrero, and J. C. Vasquez, "Distributed secondary control for islanded microgrids — a novel approach," *IEEE Trans. Power Electron.*, vol. 29, no. 2, pp. 1018–1031, Feb. 2014.
- [17] A. Bidram, A. Davoudi, F. L. Lewis, and J. M. Guerrero, "Distributed cooperative secondary control of microgrids using feedback linearization," *IEEE Trans. Power Syst.*, vol. 28, no. 3, pp. 3462–3470, Aug. 2013.
- [18] N. M. Dehkordi, N. Sadati, and M. Hamzeh, "Fully distributed cooperative secondary frequency and voltage control of islanded microgrids," *IEEE Trans. Energy Convers.*, vol. 32, no. 2, pp. 675–685, Jun. 2017.
- [19] J. Lai, H. Zhou, X. Lu, X. Yu, and W. Hu, "Droop-based distributed cooperative control for microgrids with time-varying delays," *IEEE Trans. Smart Grid*, vol. 7, no. 4, pp. 1775–1789, Jul. 2016.
- [20] X. Lu, X. Yu, J. Lai, J. M. Guerrero, and H. Zhou, "Distributed secondary voltage and frequency control for islanded microgrids with uncertain communication links," *IEEE Trans. Ind. Informat.*, vol. 13, no. 2, pp. 448–460, 2017.
- [21] S. Liu, X. Wang, and P. X. Liu, "Impact of communication delays on secondary frequency control in an islanded microgrid," *IEEE Trans. Ind. Electron.*, vol. 62, no. 4, pp. 2021–2031, Apr. 2015.
- [22] E. A. A. Coelho, D. Wu, J. M. Guerrero, J. C. Vasquez, T. Dragicevic, Stefanovi, and P. Popovski, "Small-signal analysis of the microgrid secondary control considering a communication time delay," *IEEE Trans. Ind. Elect.*, vol. 63, no. 10, pp. 6257–6269, Oct. 2016.
- [23] J. W. Simpson-Porco, Q. Shafiee, F. Drfler, J. C. Vasquez, J. M. Guerrero, and F. Bullo, "Secondary frequency and voltage control of islanded microgrids via distributed averaging," *IEEE Trans. Ind. Electron.*, vol. 62, no. 11, pp. 7025–7038, Nov. 2015.
- [24] N. M. Dehkordi, H. R. Baghaee, N. Sadati, and J. M. Guerrero, "Distributed noise-resilient secondary voltage and frequency control for islanded microgrids," *IEEE Trans. Smart Grid*, pp. 1–1, 2018.
- [25] A. Afshari, M. Karrari, H. R. Baghaee, and G. B. Gharehpetian, "Resilient cooperative control of AC microgrids considering relative state-dependent noises and communication time-delays," *IET Renewable Power Generation*, feb 2020.
- [26] —, "Distributed fault-tolerant voltage/frequency synchronization in autonomous AC microgrids," *IEEE Trans. on Power Systems*, pp. 1–15, Feb. 2020.
- [27] N. M. Dehkordi, N. Sadati, and M. Hamzeh, "Distributed robust finite-time secondary voltage and frequency control of islanded microgrids," *IEEE Trans. Power Syst.*, vol. 32, no. 5, pp. 3648–3659, Sep. 2017.
- [28] J. Lai, X. Lu, and X. Yu, "Stochastic distributed frequency and load sharing control for microgrids with communication delays," *IEEE Syst. J.*, vol. 13, no. 4, pp. 4269–4280, 2019.
- [29] J. Lai, X. Lu, A. Monti, and G.-P. Liu, "Stochastic distributed pinning control for co-multi-inverter networks with a virtual leader," *IEEE Trans. Circuits Syst., II, Exp. Briefs*, 2019, to be published, doi: 10.1109/TC-SII.2019.2950764.
- [30] A. Afshari, M. Karrari, H. R. Baghaee, G. Gharehpetian, and S. Karrari, "Cooperative fault-tolerant control of microgrids under switching communication topology," *IEEE Trans. Smart Grid*, 2019, to be published, doi: 10.1109/TSG.2019.2944768.
- [31] M. A. Shahab, S. B. Mozafari, S. Soleymani, N. Mahdian, H. Mohamadnezhad, and J. M. Guerrero, "Stochastic consensus-based control of  $\mu$ gs with communication delays and noises," *IEEE Trans. Power Syst.*, pp. 1–1, 2019.
- [32] J. Proakis and M. Salehi, *Digital Communications*. New York, NY, USA: McGraw-Hill, 2008.
- [33] J. Liu, X. Liu, W.-C. Xie, and H. Zhang, "Stochastic consensus seeking with communication delays," *Automatica*, vol. 47, no. 12, pp. 2689 – 2696, 2011.

- [34] T. Dragicevic, J. M. Guerrero, J. C. Vasquez, and D. Skrlec, "Supervisory control of an adaptive-droop regulated DC microgrid with battery management capability," *IEEE Transactions on Power Electronics*, vol. 29, no. 2, pp. 695–706, feb 2014.
- [35] M. Hamzeh, H. Karimi, and H. Mokhtari, "Harmonic and negative-sequence current control in an islanded multi-bus MV microgrid," *IEEE Transactions on Smart Grid*, vol. 5, no. 1, pp. 167–176, jan 2014.
- [36] A. Ghazanfari, M. Hamzeh, H. Mokhtari, and H. Karimi, "Active power management of multihybrid fuel cell/supercapacitor power conversion system in a medium voltage microgrid," *IEEE Transactions on Smart Grid*, vol. 3, no. 4, pp. 1903–1910, dec 2012.
- [37] M. Patzold, *Mobile Fading Channels*. John Wiley & Sons, 2002.
- [38] A. Parizad, H. R. Baghaee, G. B. Gharehpetian, and A. Yazdani, "RTISim: A new real-time isolated simulator for turbine-governor system of industrial power plants," in *IEEE International Conference on Environment and Electrical Engineering and 2018 IEEE Industrial and Commercial Power Systems Europe (EEEIC / I&CPS Europe)*. IEEE, Jun. 2018, pp. 1–6.
- [39] A. Bidram, F. L. Lewis, and A. Davoudi, "Distributed control systems for small-scale power networks: Using multiagent cooperative control theory," *IEEE Control Systems*, vol. 34, no. 6, pp. 56–77, Dec. 2014.
- [40] Q. Yang, J. A. Barria, and T. C. Green, "Communication infrastructures for distributed control of power distribution networks," *IEEE Transactions on Industrial Informatics*, vol. 7, no. 2, pp. 316–327, may 2011.
- [41] A. Goldsmith, *Wireless Communications*. Stanford University, 2005.
- [42] D. Revuz and M. Yor, "Continuous martingales and brownian motion," in *Springer Verlag*, 1999.